Available online at www.sciencedirect.com
SCIENCE DIRECT
Thermochimica Acta 414 (2004) 255–261
thermochimica acta
www.elsevier.com/locate/tca

Analysis of the area of material really tested by TMA

J. Zielnica [a], P. Wasilewicz [a], B. Jurkowski [b,*], B. Jurkowska [c]

[a] *Institute of Applied Mechanics, Poznan University of Technology, Piotrowo 3, 61-138 Poznan, Poland*
[b] *Plastic and Rubber Processing Division, Institute of Material Technology, Poznan University of Technology, Piotrowo 3, 61-138 Poznan, Poland*
[c] *Research and Development Centre for the Tire Industry (OBRPO) Stomil, 61-361 Poznan, Starolecka 18, Poland*

Received 7 January 2004; received in revised form 8 January 2004; accepted 8 January 2004

Abstract

Deformation distribution within the specimen beneath the thermomechanical analysis (TMA) probe, found by using the finite element method (FEM), depends mainly on penetration depth, specimen thickness and diameter as well as on radius of the probe tip when the Poisson's ratio influences it just slightly. For standard radius of the tip $R_o = 1$ mm, most deformation is distributed in a material layer up to 0.5 mm thick independently on elastic modulus of a polymer at a glassy state. It is caused by the fact that maximal penetration depth for the polymers usually equals to about 0.05 mm. Because of this, the contact surface area is less than 0.17 mm^2 for the standard radius of the tip. This evidences that predominantly the specimen volume equal to 0.5 mm × 0.17 mm^2 (depth × area) is tested by the TMA at compression mode. For $R_o = 5$ mm is tested the layer 2.5 mm thick. This makes possible to evaluate the material properties in the zone of different thickness depending on radius of the tip.

Keywords: Thermomechanical analysis; Finite element method; Rubber; Engineering plastics; Skin properties

1. Introduction

The thermomechanical analysis (TMA) is based on measurements of the specimen's deformation under very low load at scanned temperature giving the thermomechanical curve (TMC) [1–4]. It allows the evaluation of the glass transition temperature [5–7], which is higher than that determined by positron annihilation spectroscopy (PALS) [8] and DSC [9], but a little lower than that determined by DMA [9]. In many cases, transition temperatures from TMA suit well to those found by other techniques [10]. In addition, the thermal expansion coefficient [9,11–13], the softening temperature [14] and, according to some scientists, both the crosslinking degree (based on equilibrium elastic modulus) [15,16], and the average number of degrees of freedom of polymer segments between crosslinks [17] could be evaluated by TMA. Thermomechanical contribution, which is due to a variable physical contact area for a probe tip, is dominant in the microthermal response of polymers [18]. It means that TMA is commonly used till now in the polymer processing industry in spite of some limitations [19,20], which are also related with the loading conditions [21] and some uncertainty of the area of materials really tested.

The TMC could be approximated as lines with several breaks separating the apparently linear segments with varied slopes, what informs about an existence of material regions with different thermal expansion properties. It is assumed that they have very complex structures, including higher-level arrangement than molecular one. From this curve, it is possible to evaluate the transition temperatures. Morphology with two or three amorphous regions, most likely interpenetrating, and more ordered portion for the studied polymers has been found by using a novel version of TMA [22]. These regions are not divided in space; they represent several types of interactions, which coexist in polymers. They differ in the transition temperatures up to 200 °C and related interaction energies equal to kT (k is Boltzmann's constant and T is temperature) as well as compactness, what should influence the distribution of additives within the polymer matrix.

In order to evaluate the equilibrium elastic modulus E_∞, and to locate the plateau of high-elasticity as accurate as possible by using the TMA device, the measuring of specimen's thermal expansion at compression mode has to be done at

* Corresponding author. Tel.: +48-61-6652-776; fax: +48-61-6652-217.
E-mail address: boleslaw.jurkowski@put.poznan.pl (B. Jurkowski).

0040-6031/$ – see front matter © 2004 Elsevier B.V. All rights reserved.
doi:10.1016/j.tca.2004.01.012

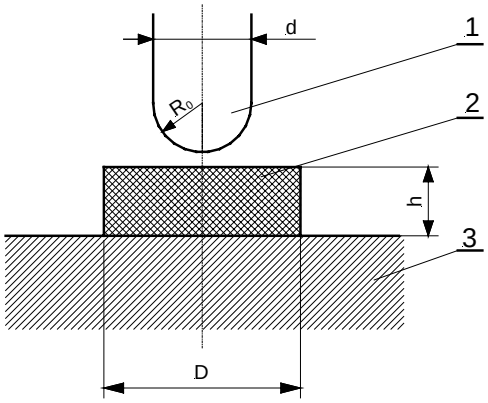

Fig. 1. Schematic illustration of the TMA testing device: 1, probe hemispherical tip; 2, specimen; 3, base.

low load. The deformation should be kept within the range of polymer elasticity. This deformation should not exceed 5% of the radius of a probe with a hemispherical tip, usually $R_o = 1$ mm (Fig. 1); it is measured with accuracy of 5 nm [23]. Usually, the probe of 2 mm in diameter is made of quartz—the material with much higher elastic modulus and very low coefficient of thermal expansion when compared to the tested specimen. The contact surface area between the probe and the specimen varies from almost point (at a glassy state) up to approximately 0.17 mm^2 (at rubbery or visco-elastic states). It means that the information about polymer properties on this varied area is averaged. Simultaneously, for the thinnest PS film with clearly detectable response (25 nm), the glass transition temperature is 20 °C below its bulk value [24] what suggests some differences to appear in a structure of successive material layers. This fact evidences that it is very important to know how thick polymer layer is really tested by TMA.

Cubic or cylindrical specimens of 1.2–5 mm in height and 1–5 mm in width or diameter (preferably 1.5 and 2 mm, respectively) are used for measurements at compression mode. These specimens are moulded or cut from the plates of the polymeric material. Surfaces contacting the base of the thermostatic chamber of the instrument and a measuring probe should be parallel each other.

The TMA methodology is based on a simplified model of polymer network with physical junctions and/or chemical crosslinks. Polymers are tested in solid state and visco-elastic state, what is described in detail elsewhere [22,23,25]. This methodology reduces most of limitations of generally used previous version [1–4], but it is not proved sufficiently till now. Because of this, the aim of current work is to make some progress in this area.

The thickness of really tested polymer layer determines also the characteristics of molecular and topological structures evaluated by the novel version of TMA [22]. To date, however, we did not found any reliable information about its evaluation. Finding it is a fundamental problem because for semi-crystalline materials and filled composites, the structure of successive layers of the specimen varies depending on their location toward outer surface, and it depends on conditions of the specimen manufacturing.

Some researches believe that TMA evaluates the averaged characteristics of the all specimen [22,23]. Other supposes that only a skin layer of the specimen is tested. Basing on continuous mechanics, it is expected that distribution of deformation when the TMA probe contacts the specimen depends on physical properties of the material, especially on its elastic modulus, the Poisson's ratio, and spectrum of relaxation times. In order to determine the thickness of polymer layer really tested both Hertz equation and, next, computer simulation based on the finite element method (FEM) has been used and the results are described below.

2. Numerical experiments

2.1. Materials and loading conditions

Elastic modulus for polymeric materials usually varies from 2 MPa (in a high-elastic state) to 3000 MPa (in a glassy state), and the Poisson's ratio varies from 0.3 to 0.5. Also, in the calculations it was accepted that the size of cylindrical specimens was assumed to be 1 or 3 mm in height and 3 or 5 mm in diameter, respectively. The measuring probe should compress the specimen along their common axis. The radius of the probe tip used in the calculations was equal to 1 (standard), 2 or 5 mm, respectively.

2.2. Methodology

To calculate elastic modulus E based on penetration depth H of the TMA probe, Hertz equation has been used [25–28]:

$$E = \frac{3(1-\nu^2)P}{4R_o^{1/2}H^{3/2}} \quad (1)$$

where ν is the Poisson's ratio; P, the load; and R_o is the radius of the hemispherical tip of the probe.

In order to determine the distribution of local deformation in the specimen beneath the probe, the FEM [28] has been applied. This numerical method is often used for the approximate solution of complex engineering and scientific problems. The basic idea of the method is to find a solution of a complicated problem by replacing it by a simpler one. The region of solution is considered as built up of many small, interconnected sub-regions called finite elements. In each element, a convenient approximate solution is assumed and the conditions of overall equilibrium of the structure are derived. The satisfaction of these conditions will yield an approximate solution for the deformation and stresses. Moreover, FEM analysis provides a very controlled manner of evaluating the force–distance response for various types of hard/soft domain/matrix combinations. Also, various geometries of probe tip can be

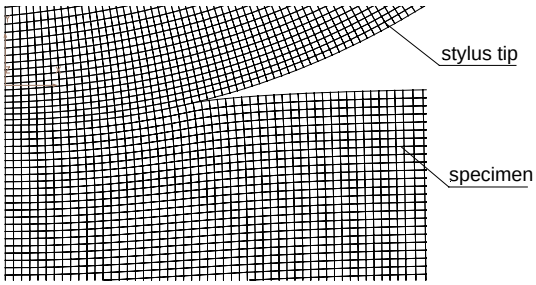

Fig. 2. Deformation of the specimen beneath the quartz probe tip with radius $R_o = 1$ mm, probe displacement 0.05 mm, elastic modulus of the probe 94,000 MPa, elastic modulus of the specimen 360 MPa.

evaluated, except for the case of an infinitely sharp indenter; the resulting point contact loading causes numerical instabilities in the finite element solution. In the considered contact problem (see Fig. 1), quadrilateral and axially symmetrical finite elements have been used because of axial symmetry of the problem. The finite elements in the specimen are squares with the side equal to 0.01 mm, and the probe was meshed by the quadrilaterals shaped very close to square in the region of maximal stresses. A non-linear and iterative method with using the specific contact (gap) elements, because the discussed problem is non-linear one, has been applied. The contact area of the two bodies being in touch also varies when the applied external load is changed. Thus, the gap elements do not allow for the mutual penetration of the meshes of the two bodies. The gap elements transmit the loads between the probe and the specimen. In Fig. 2, a sectional view of deformed finite element mesh at the contact surface of the probe and the specimen is presented. Because the contact surface of the probe deflects a little, the real probe displacement is greater than that for a case of a rigid probe.

3. Results

3.1. Influence of elastic modulus and Poisson's ratio on penetration depth

To calculate radius a of a contact surface beneath a probe of the TMA device and a polymer specimen Hertz equation for elastic semi-space was used. The probe has a hemispherical tip with radius 1 mm. In Fig. 3, the radius of the contact surface was expressed as a relative value; it means it is divided by its magnitude obtained for $E = 1$ MPa, $\nu = 0$. This makes that the vertical variable in the diagram is dimensionless and the results are independent of units. The maximal displacement of the probe equals to 0.05 mm. It is seen that the changes in a relative radius of a contact surface are substantial only for elastic modulus below 1 GPa. For higher elastic modulus value, what is typical for rigid or highly filled polymers in a glassy state, this radius decreases; the ratio of such variation tends to zero for infinite value of elastic modulus. Such displacement and low magnitude of elastic modulus are usually observed at the end of high-elastic deformation of the specimen at the TMA test at compression mode. Simultaneously, one should remember that relaxation properties of the tested materials are not taken into account in well known Hertz solution of a contact problem.

The Poisson's ratio changing within the interval between 0 and 0.5 influences slightly (Fig. 3) the radius of a contact surface of the probe tip and the specimen. It evidences that for the Poisson's ratio between 0.3 and 0.5 (usually observed interval), and elastic modulus in the characteristic range for polymeric materials, there is no reason to take into account the influence of such changes on deformation distribution within the specimens tested. These calculations have been performed using Hertz solution of a contact problem with the assumption that the thickness of material layer deformed

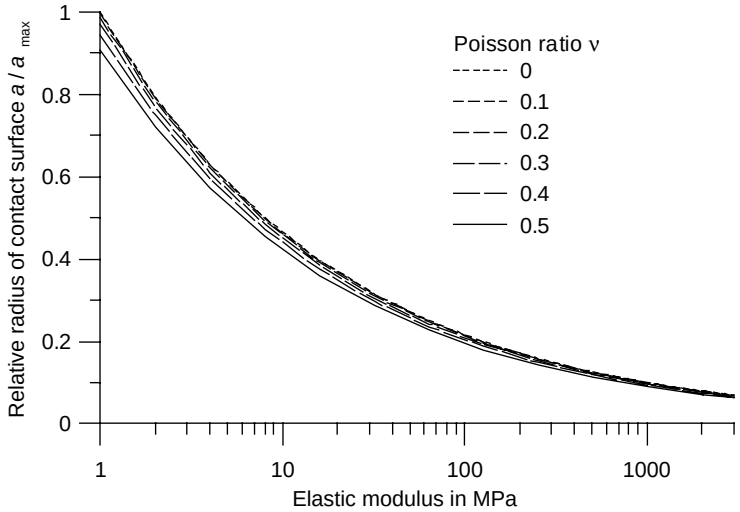

Fig. 3. Dependency of radius of the contact surface between the probe tip of the TMA device and the specimen for varied both elastic modulus and the Poisson's ratio.

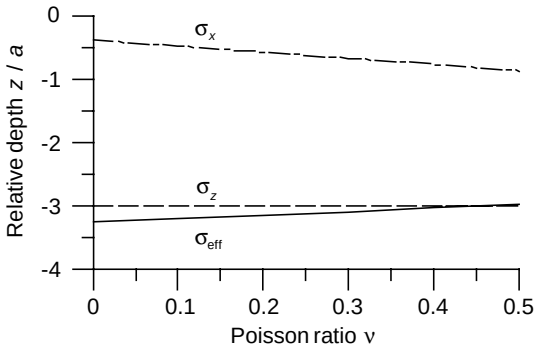

Fig. 4. Dependency of the depth beneath the centre of symmetry of a contact surface of the probe tip and specimen at which vertical σ_z, horizontal σ_x, and effective σ_{eff} stresses are reduced to 10% of maximal magnitude of σ_z on the Poisson's ratio.

by the hemispherical tip is infinitely large. However, this condition is not fulfilled for the TMA test. Because of this, some error of evaluation was introduced. In order to reduce it and to make analysis deeper, it is needed to apply the other methods, i.e. the FEM as it is presented in all Sections below.

3.2. Influence of Poisson's ratio on local stress distribution

In second simulation, it has been assumed that both thickness and diameter of the specimen are infinitely large. Radius of the probe tip R_o was chosen to be 1 mm. From calculations, it has been found (Fig. 4) that local vertical σ_z and effective σ_{eff} stresses, in rubbers and engineering plastics, beneath the contact area of the probe tip are reduced up to 10% of maximal magnitude of vertical stress σ_z at the distance z equal to about $3a$. This depth is directly proportional to radius a of a loaded surface. Horizontal stress σ_x reaches this magnitude on the depth within 0.4 and 0.8 of the radius of the contact surface. The results are low dependent on the Poisson's ratio and independent on elastic modulus.

3.3. Influence of thickness and diameter of the specimen on local deformation

In third simulation, it was assumed that radius R_o of a hemispherical probe tip equals to 1 mm and diameter d of the cylindrical specimen varies between 3 and 5 mm. Simultaneously, thickness h of the specimen equals to 1 or 3 mm, respectively. Fig. 5 shows the curves, inside which the local stresses are greater than 10% of their maximal magnitude. It is concluded from this Figure that the thickness of material layer, in which local stresses have reached the level below 10% of their maximal value at contact, is low dependent on both the thickness of the specimen varied between 1 and 3 mm and on diameter of the specimen, when it is greater than 3 mm. It evidences the fact that Hertz solution of a contact problem is close to calculations based on the FEM for the thickness of the specimen greater than 1 mm. So, we can

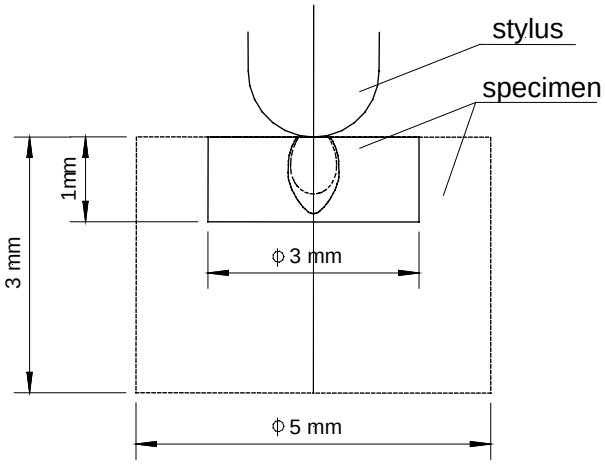

Fig. 5. Dependency of the zone in which local stresses are >10% of maximal stresses during TMA test on the size of specimen tested, calculated for $E = 360$ MPa, $\nu = 0.3$, and $R_o = 1$ mm; (—) specimen Ø3 × 1 mm and (- - -) specimen Ø5 × 3 mm.

conclude that there is no need to test the specimens with the thickness larger than 1 mm.

3.4. Influence of radius of the probe tip on local deformation distribution

Radius of the hemispherical probe tip should influence the distribution of stresses on the contact surface with the specimen. Usually, this radius equals to 1 mm. It is expected that varying this radius we can change the form of stress and deformation distribution within the contact area. From the results of fourth computer simulations with $E = 360$ MPa and $\nu = 0.3$ (Fig. 6) it is concluded that the change of radius of the probe tip from $R_o = 1$ mm (a usual case) to $R_o = 5$ mm causes that the deformation zone increases substantially. In Fig. 6, the curves, inside which the local stresses are greater than 10% of their maximal magnitude are presented. This fact that the deformation zone increases substantially makes possible to evaluate the material properties in the zone of greater thickness. For instance, in a case of

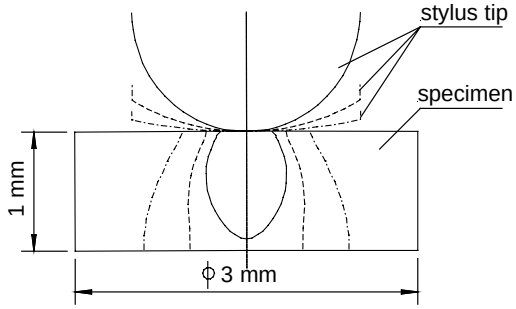

Fig. 6. Dependency of the zone of specimen 1 mm thick in which local stresses are >10% of maximal stresses during TMA test on the radius R_o of the hemispherical probe tip calculated for $E = 360$ MPa, $\nu = 0.3$, (—) $R_o = 1$ mm, (- - -) $R_o = 2$ mm, (·····) $R_o = 5$ mm.

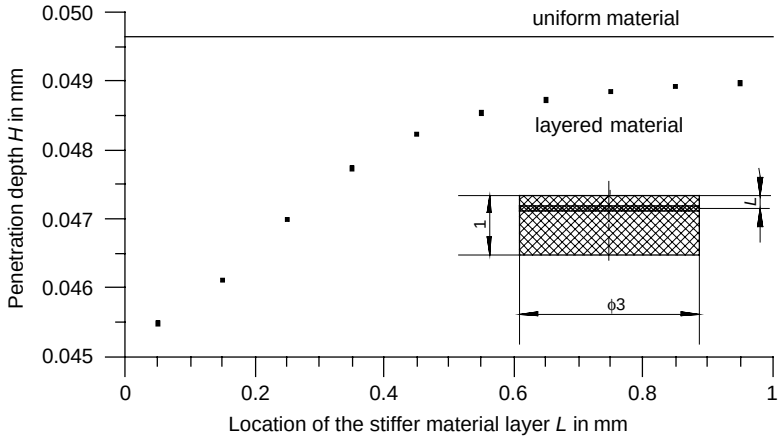

Fig. 7. Dependency of the penetration depth of the probe during TMA test on the location of the material layer with doubled elastic modulus in comparison with a surface layer calculated for $E = 360\,\text{MPa}, \nu = 0.3$, and $R_o = 1\,\text{mm}$.

$R_o = 1\,\text{mm}$, a layer of 0.5 mm thick is really tested, whereas for $R_o = 5\,\text{mm}$ such a layer is about 2.5 mm thick. The discussion above, concerns the homogeneous materials. For sandwich-like materials, which layers differ in elastic modulus (very common case), the conclusions may be different.

3.5. Influence of a gradient of elastic modulus on penetration depth

In fifth simulation, it was assumed that radius of the probe tip equals to $R_o = 1\,\text{mm}$, the specimen is 1 mm thick and it consists of 10 layers of 0.1 mm thickness each. Calculations were performed under the assumption that one layer located in different distance from the surface has elastic modulus twice larger than other layers. Constituency of the tested material (Fig. 7) up to 0.5 mm of specimen thickness (about two radii of the probe tip) expresses the fact that the location of more rigid layer substantially influences the penetration depth of the probe. Simultaneously, location of such rigid layer between 0.5 and 1.0 mm from the loaded surface of the sandwich-like specimen less influences the penetration of the probe when compared with a case of homogenous material. It means that the TMA is sensitive to differences in elastic properties of the material if tested in a layer up to 0.5 mm thick only.

Next, a two-ply specimen has been analysed where the elastic modulus of the lower layer is twice as large as that for the upper one in contrast to the previous discrete results presented in Fig. 7. Here, a non-linear numerical simulation, using the FEM has been performed, basing on the modified

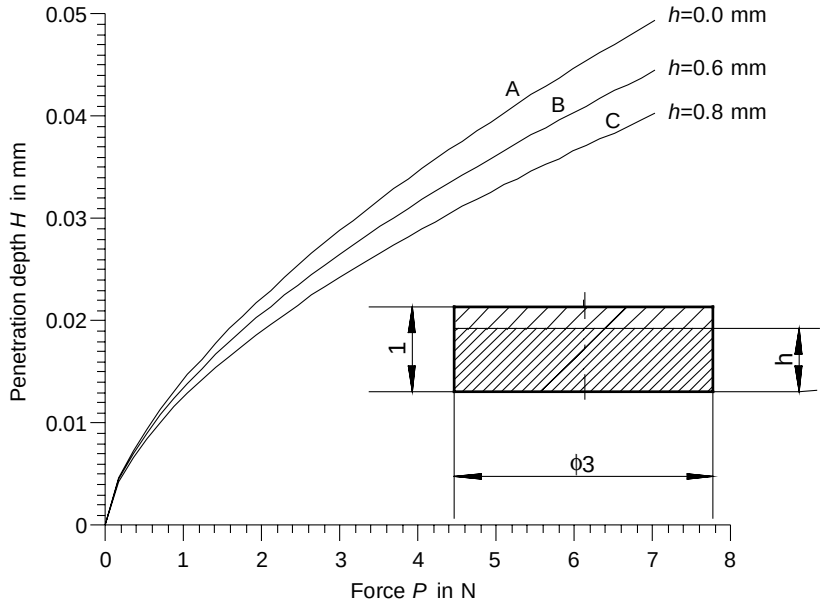

Fig. 8. Relation between the penetration depth H of the probe and applied force P for two-ply specimen. $E_{\text{upper layer}} = 360\,\text{MPa}$, $E_{\text{lower layer}} = 720\,\text{MPa}$, $\nu = 0.3$, $R_o = 1\,\text{mm}$.

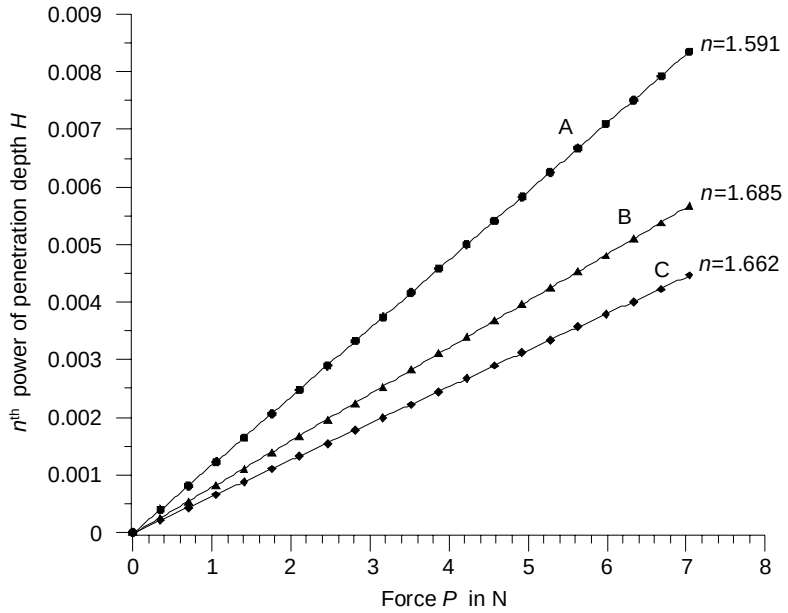

Fig. 9. Results of computer simulation by the finite element method aiming the determination of the exponent at the penetration depth H in order to get a linear relation between H and P; case A, a single layer specimen; case B, when $h = 0.6$ mm, and case C, when $h = 0.8$ mm.

Newton–Raphson procedure (40 steps of increment of load control parameter). Fig. 8 shows a relation between penetration depth H of the probe and the applied axial load P at different thickness of the lower layer. The curve A ($h = 0.0$ mm) corresponds to the presentation given in Fig. 1. As one can see, the sub-dividing of the specimen into two layers, where lower one has higher elastic modulus, results in a greater total rigidity of the specimen. The deformation developed by the same load is less then that of a single-layer specimen. The greater thickness h of lower layer the higher is rigidity of the specimen.

The objective of a final investigation is analytical (by Hertz method) and numerical (by the FEM) evaluation of the relation between penetration depth H of the probe and the applied load P. The rearrangement of formula (1) gives

$$H^n = \frac{3(1-\nu^2)P}{4R_o^{1/2}E}, \quad n = \frac{3}{2} \tag{2}$$

It is obvious that the relation between penetration depth H and force P is non-linear one. Now the problem is: what should be the value of the exponent at H in order to get a linear relation between H^n and P. This exponent (denoted n) is a measure of the differences between the analytical solution by Hertz method (infinite elastic half-space) and numerical solution by the FEM, where the considered specimen has a limited size. Fig. 9 presents the same results as just discussed in Fig. 8, but now the vertical axis is H^n (it was H in Fig. 8). Exponent n has been evaluated under condition that the correlation coefficient between H^n and P should be not less than 0.9999. In this case, the curves in Fig. 9 are linearized. The following results have been obtained: $n = 1.591$ (case A, a single layer specimen), $n = 1.662$ (case B, when $h = 0.6$ mm), and $n = 1.685$ (case C, when $h = 0.8$ mm). It means that the higher is coefficient n the higher is the gradient of elastic modulus along the depth of the specimen. Coefficient n for case A is greater than $n = 1.5$ in Hertz formula. This can be justified by the influence of the boundary conditions at the model outer surfaces, which otherwise, does not exist in Hertz solution. The n exponent is much greater for cases B and C then that for case A, what could result from the actual structure of the tested material.

4. Conclusions

Application of the FEM models with the considered geometries show that it is not possible for TMA testing to resolve features smaller than the radius of the tip by force imaging. The analyses show that when such a domain of specimen size is large enough to be resolved, its effect is limited to a region surrounding the domain. These analyses define limitations on the depth and lateral distance away from the point of indentation at which such domains can be detected by the method.

The zone of deformation distribution beneath the TMA probe tip contacting the specimen depends substantially on elastic modulus of the tested material and only a little on Poisson's ratio. It has been calculated that most of deformation is localized within a layer of material with thickness equal up to two radii of the contact surface area. It means that in the beginning of TMA test at compression mode, when the elastic modulus is high (low temperature), the layer of the tested material is very thin, and with temperature rise it gets thicker up to 0.5 mm when a polymer is in a high-elastic state. It has been accepted that maximal penetration depth for all tested materials equals to about 0.05 mm. Because of

this, the contact surface area is less than $0.17\,mm^2$ for the standard radius of the probe. However, the area is proportional to the radius R_o of the probe tip for greater radii at constant penetration depth. The influence of specimen thickness and diameter on the deformation distribution is small.

For $R_o = 5\,mm$ the deformation zone increases substantially in comparison with the case of $R_o = 1\,mm$. This makes possible to evaluate the material properties in the zone of greater thickness when using greater radius of the tip.

References

[1] B. Wunderlich, Thermal Analysis, Academic Press, New York, New Jersey, 1990.
[2] T. Hatakeyama, F.X. Quin, Thermal Analysis, Wiley, Chichester, UK, 1994.
[3] B.Y. Teitelbaum, Thermomechanical Analysis of Polymers (in Russian), Moscow Nauka Publishers, 1979.
[4] D.M. Price, M. Reading, T.J. Levar, J. Thermal Anal. Calorimetry 56 (2) (1999) 673–679.
[5] D.Y. Tang, W.M. Qin, W.M. Cai, L. Zhao, Mater. Chem. Phys. 82 (1) (2003) 73–77.
[6] K. Kurschnar, P. Strokriegl, P. Van de Vitte, Lub. J. Mol. Crystals 352 (2000) 735–744.
[7] J.W. Schultz, R.T. Pogue, R.P. Chartoff, J.S. Ullett, J. Thermal Anal. 49 (1) (1997) 155–160.
[8] T. Suzuki, T. Hayashi, Y. Ito, Mater. Res. Innovations 4 (5–6) (2001) 273–277.
[9] C.S. Wang, T.S. Leu, Polymer 41 (10) (2000) 3581–3591.
[10] W. Brostow, E.A. Faitelson, M.G. Kamensky, V.P. Korkhov, Y.P. Rodin, Polymer 40 (6) (1999) 1441–1449.
[11] T.S. Leu, C.S. Wang, Polymer 43 (25) (2002) 7069–7074.
[12] B. Nandau, K.N. Pandey, G.D. Pandey, A. Singh, L.D. Kandpal, G.N. Mathur, J. Thermal Anal. 64 (2) (2001) 529–537.
[13] H. Tang, X.G. Chen, Y.X. Luo, Eur. Polym. J. 33 (8) (1997) 1383–1386.
[14] S.H. Hsiao, C.T. Li, J. Polym. Sci. Polym. Chem. 37 (10) (1999) 1435–1442.
[15] C. Konetschny, D. Galusek, S. Reschke, C. Fasel, R. Riedel, J. Eur. Ceram. Soc. 9 (16) (1999) 2789–2796.
[16] Y.I. Matusevich, A.P. Polikarpov, L.P. Krul, High-Energy Chem. 33 (4) (1999) 224–228.
[17] A. Pizzi, R. Garcia, S. Wang, J. Appl. Polym. Sci. 66 (2) (1997) 255–266.
[18] V.V. Tsukruk, V.V. Gorbunov, N. Fuchigarni, Thermochim. Acta 395 (1–2) (2003) 151–158.
[19] R. Garcia, A. Pizzi, J. Appl. Polym. Sci. 70 (6) (1998) 1093–1109.
[20] R. Garcia, A. Pizzi, J. Appl. Polym. Sci. 70 (6) (1998) 1111–1119.
[21] K. Nakamura, E. Kinoshita, T. Hatakeyama, H. Hatakeyama, Thermochim. Acta 352 (2000) 171–176.
[22] B. Jurkowska, Y.A. Olkhov, B. Jurkowski, J. Appl. Polym. Sci. 74 (3) (1999) 490.
[23] Y.A. Olkhov, V.I. Irzhak, S.M. Baturin, RU Patent 2023255 (1989).
[24] V.V. Gorbunov, N. Fuchigarni, V.V. Tsukruk, High Perform. Polym. 12 (2000) 1–8.
[25] Y.A. Olkhov, B. Jurkowski, B. Jurkowska, Eur. Polymer J., in preparation.
[26] J.M. Gere, S.P. Timoshenko, Mechanics of Materials, second ed., PWS-Kent Pub. Company, Boston, 1994.
[27] J.M. Barton, Anal. Proc. 8 (10) (1981) 411.
[28] S.S. Rao, The Finite Element Method in Engineering, Pergamon Press, New York, 1989.